Measurements of uv two-photon absorption relative to known Raman cross sections

Yehiam Prior* and Hans Vogt†
Gordon McKay Laboratory, Harvard University, Cambridge, Massachusetts 02138
(Received 16 November 1978)

Two-photon absorption (TPA) cross sections of benzene and of three alkali-halide crystals (KI, KBr, RbBr) are reported for a total excitation energy of 6.7 eV. A calibration technique is used whereby the TPA coefficient at the sum frequency $\omega_P + \omega_L$ of two interacting laser beams at ω_P and ω_L is compared to the known stimulated Raman gain at the difference frequency $\omega_L - \omega_P$ in the same material, or in other materials. The results, obtained with nsec pulses, are compared to cross sections measured by a psec laser system. A proposal is made for the extension of the present experimental setup, resulting in a significant enhancement in sensitivity and the possible utilization of low-power cw lasers for these measurements.

I. INTRODUCTION

The two-photon absorption (TPA) process—in which two photons are simultaneously absorbed by a material without an intermediate level to match either one of the photons—was observed as early as 1961 by Kaiser and Garrett.[1] In their original experiment these authors irradiated a CaF_2 crystal doped with Eu^{2+} by a strong pulse of red light from a ruby laser and observed the blue fluorescence that followed the absorption of two red photons by the rare-earth ions. Many other experiments were reported where different physical effects were used to observe TPA. Thermal lensing in liquids,[2] multiphoton ionization in gases,[3] and TPA free-carrier generation in solids,[4] to mention a few, were all used to study TPA spectra. In order to derive absolute values from the direct measurements, a large number of parameters had to be known to a high degree of accuracy. Some of these parameters like laser power, beam profile, mode structure, and beams overlap, are difficult to measure, while others like hot spots in the beam are impossible to determine. Thus in all these experiments only relative information on the TPA cross sections could be obtained. The reader is referred to several articles for a review of TPA.[5]

More recently, several techniques have been reported for the determination of absolute cross sections. These experiments, like any other absolute cross-section measurement, are difficult to perform, especially so due to the dependence of the measured effect on the laser parameters. Two approaches were used: in the first approach[6-8] the attenuation of the laser beam due to two-photon absorption in the sample was directly monitored. Because of the stringent requirements for exact knowledge of the spatial and temporal profile of the laser pulses and the geometrical factors of the experimental setup, and because of the need for absolute calibration of all the measuring devices, this approach was limited to a single laser system—a mode-locked Nd-YAlG laser—over the very limited spectral range of the fundamental laser wavelength at 1.06 μm and its higher harmonics. In the second approach[9-13] a measurement was performed in which the TPA coefficient was compared to other nonlinear parameters of the same material or other materials. By the use of the well developed theory of nonlinear optics, absolute TPA coefficients were obtained from absolute Raman cross sections measured in spontaneous Raman scattering experiments. In a way, this indirect method is not an absolute measurement, as it relies on the availability of absolute Raman cross sections for its calibration.

In the present paper we extend the work of deAraujo and Lotem[13] to the uv range. By means of internal calibration (comparison of TPA and Raman cross section in the same material) we obtain absolute TPA cross sections of benzene at 6.7 eV. In addition we report the results of TPA cross sections of several alkali-halide crystals at the same energy range.

It should be pointed out that neither the direct measurement nor the present method is sensitive to the difference between true TPA and a stepwise process. Only the parametric method,[10] where the contributions to the imaginary part of $\chi^{(3)}$ from two different resonances (TPA and Raman) interfere, is capable of distinguishing between the two.

The relations between TPA and Raman processes and the third-order nonlinear susceptibility are briefly reviewed in Sec. II. The experimental procedure and setup are described in Sec. III, while the results are presented and analyzed in Sec. IV. The results are discussed and compared to other published data, and an extension of this method is proposed. The procedure for determination of the absolute Raman cross section is given in the Appendix.

II. THEORY

Consider the interaction of two beams, a strong laser beam of frequency ω_L and intensity I_L, and a weak probe beam of frequency ω_P and intensity I_P. The change in intensity of the probe beam can be written

$$\frac{\partial I_P}{\partial z} = -\alpha_P I_P - \beta I_P I_L , \tag{1}$$

where z is the direction of propagation of the beams in the sample, α_P is the linear absorption coefficient at ω_P, and β is the TPA coefficient at $\omega_P + \omega_L$ induced by the presence of I_L. For the case of parallel beam polarizations, β is related to the third-order nonlinear susceptibility by[7]

$$\beta = (32\pi^2\omega_P/c^2 n_P n_L)[6\chi''_{xxxx}(-\omega_P, \omega_P, \omega_L, -\omega_L)] . \tag{2a}$$

n_P and n_L are the refractive indices at ω_P and ω_L, and c is the speed of light.

The factor of 6 comes from the conventional definition of $\chi^{(3)}(-\omega_P, \omega_P, \omega_L, -\omega_L)$, and is the actual number of permutations possible between the input frequencies: ω_P, ω_L, $-\omega_L$. For the case of only one frequency being involved, the three input frequencies are ω_L, ω_L, $-\omega_L$, and the corresponding factor is 3. These numerical factors will be important when the results of two such experiments are compared.

In Eq. (1) both I_P and I_L are, in general, dependent on the transverse-mode structure and temporal profile of the lasers. Thus the absorption will depend on the complicated overlap integral

$$\int\int\int dx\,dy\,dt\, I_P(x,y,z,t)\, I_L(x,y,z,t)$$

instead of the simple product $I_P I_L$. As these functions are not in general known for high power pulsed lasers, it is clear why attempts to obtain accurate cross sections from direct measurements with such lasers led to large scatter of results.[5]

As the coefficient β is proportional to $\chi^{(3)}(-\omega_P, \omega_P, \omega_L, -\omega_L)$ it will respond to all resonance enhancements in this quantity. These occur not only when the sum $\omega_L + \omega_P$ is near a two-photon absorption region, but also when the difference $\omega_L - \omega_P$ is near the frequency of a Raman-active mode. Hence β may be written

$$\beta = \beta_T - \beta_R , \tag{2b}$$

where β_T and β_R represent the TPA and Raman contribution, respectively, and the negative sign indicates an amplification of the probe beam at the Raman resonance.

Since in our measurements we eventually compared TPA in a crystal to Raman gain in a liquid, a formula will be derived for the case of a crystal immersed in a liquid cell. Consider a crystal of length l in a liquid cell of length d. The distance between the crystal and the front window of the cell is d_1, and that between the crystal and the back window of the cell is d_2, so that $d = d_1 + d_2 + l$. With the definitions R is the reflection loss at the windows and r is the reflection loss at the crystal-liquid face, the intensity at the output of the composite sample cell is given by the general formula

$$I_P(d) = (1-R_P)^2(1-r_P)^2 I_P(0) \times \exp[-\alpha_{P,l}(d_1+d_2) - \beta_{\text{eff}} I_L(0) d] , \tag{3}$$

where

$$\beta_{\text{eff}} = (1/d)\{\beta_{T,c}\alpha_{L,c}^{-1}(1-R_L)(1-r_L)(1-e^{-\alpha_{L,c}l})e^{-\alpha_{L,l}d_1} + (\beta_{T,l}-\beta_{R,l})(1-R_L)\alpha_{L,l}^{-1}[(1-e^{-\alpha_{L,l}d_1}) + (1-r_L)^2 e^{-\alpha_{L,l}d_1 - \alpha_{L,c}l}(1-e^{-\alpha_{L,l}d_2})]\} . \tag{4}$$

The subscripts P and L refer to the probe and laser frequencies, respectively, and the second subscript l and c refer to the liquid and crystal sections of the cell. $I(0)$ is the incident intensity. The assumption is made that Raman gain exists only in the liquid, whereas TPA is present in both the liquid and the crystal.

Equation (3) is a careful solution of the differential equation (1) in sections, taking into account all linear and nonlinear losses, except the depletion of I_L by TPA. The following assumptions lead to a significant simplification: (a) Linear absorption can be neglected. Since there are no one-photon resonances at ω_P and ω_L, and these photon energies are much less than the band gap in the crystals, the error involved in this approximation is negligible. This assumption is especially valid as there are liquid sections on both sides of the crystal. (b) Since the crystals are immersed in the liquid, we have a near index match, and reflection losses at the crystal-liquid surface can be neglected. In addition, scratches and other crystal surface imperfections which might otherwise cause scattering and reduction in the intensity of the beams are far less important than for the case of a crystal in air.

Under (a) and (b), the probe beam intensity at the output of the cell is

$$I_P(d) = (1-R_P)^2 I_P(0) e^{-\beta_{\text{eff}} I_L(0) d} , \tag{5}$$

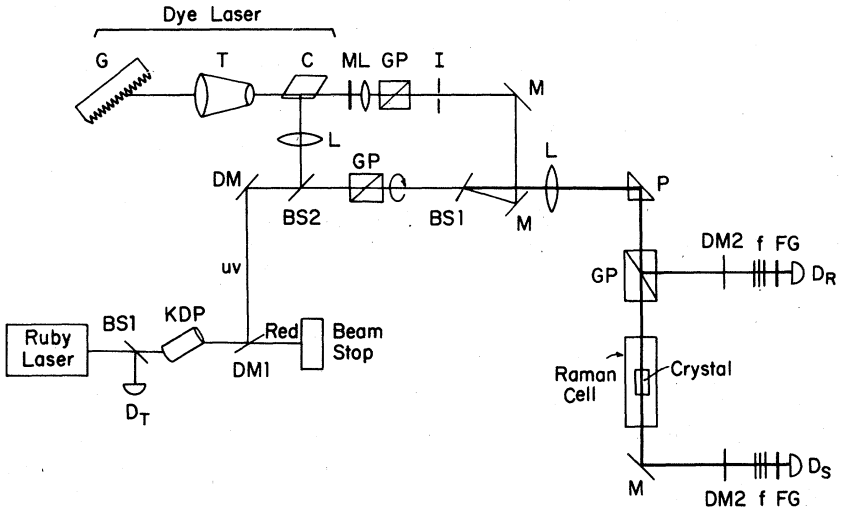

FIG. 1. Scheme of the experimental arrangement for the TPA measurement. M - mirror; DM - dichroic mirror; BS - beam splitter; GP - Glan prism; C - dye cell; T - telescope; G - grating; L - lens; P - prism; f - filter; FG - frosted glass; D_R, D_S - photodiode; D_T - triggering diode; KDP - frequency doubling crystal.

with

$$\beta_{\text{eff}}=(1/d)[\beta_{T,c}l+(\beta_{T,l}-\beta_{R,l})(d-l)](1-R_L)\,. \tag{6}$$

Unfortunately, β_R is not the quantity that is usually quoted in measurements of Raman cross sections. The measured quantity is $d\sigma/d\Omega$ which is the differential cross section for spontaneous Raman scattering into a solid angle $d\Omega$, with the polarizations of the incident and scattered light parallel, integrated over the entire Raman line profile. The gain for the stimulated Raman effect is given in terms of this quantity[14]:

$$g(\omega_P)=\beta_R I_L=\frac{8\pi^3c^2}{\hbar n_P^2}\,\frac{1}{\omega_L\omega_P^2}\,\frac{N}{V}\left(\frac{d\sigma}{d\Omega}\right)_{\!\parallel} S(\omega_P)I_L\,, \tag{7}$$

where N/V is the molecular density of the sample, $S(\omega_P)$ is the normalized line-shape function of the Raman line, i.e., $\int S(\omega_P)d\omega_P=1$. A thermal factor taking into account the occupation of the upper level of the Raman transition has been omitted.

It should be restated that the purpose of this calculation is to obtain a relation between the Raman gain and the TPA loss experienced by the probe beam upon traversing the composite sample. Equation (7) expresses β_R in terms of $(d\sigma/d\Omega)_{\parallel}$, and from Eqs. (2) β_T can be found.

III. EXPERIMENTAL SETUP

The experimental setup used in these experiments is described schematically in Fig. 1. The short intense pulse (20 nsec, 10 MW) of a Q-switched multimode Raytheon ruby laser, is doubled in a potassium dihydrogen phosphate (KDP) angle tuned crystal (15 nsec, 1 MW at 347.1 nm) with efficiency of about 10%. The uv light is separated from the red by two dichroic mirrors and sent through a rotatable Glan prism polarizer, a lens, and a second Glan prism to the composite sample. BS2 splits off about 20% of the uv beam to pump a Hänsch-type dye laser. In these experiments, we used a solution of the dye Pilot 386, a proprietary Oligo-Phenylene manufactured by New England Nuclear, in a 50% mixture of ethanol and toluene, and obtained good lasing in the range 380–392 nm with laser linewidth of about 0.5 cm^{-1}. The dye laser or "probe" beam is collimated and stopped down, and by means of BS1 (a glass slide) is sent collinearly with the strong light at 347.1 nm (the "laser beam") through a second Glan prism to the composite sample. The second Glan prism splits off part of the two beams into the detector D_R. The dichroic mirror DM2, which passes light at frequency ω_P but blocks frequency ω_L, and the set of colored glass cut-off filters discriminate against ω_L, and insure that the detector sees only the light at ω_P. The frosted glass serves to uniformly illuminate the 2-in. diameter biplanar ITT F4000 photodiode, to reduce shot to shot fluctuations. The beams traverse the composite sample and enter the signal channel, which is identical in its construction to the reference channel. In order to insure uniform frequency response over the measured range, the channels are optically identical. The signals from the photodiodes are amplified, digitized, and analyzed on a computer as described in a previous paper.[11] The signal and reference channels are used as a standard normalization procedure to correct for shot to shot amplitude fluctuation in the dye laser.

At a given intensity I_L (second harmonic of the ruby) which is determined by the rotatable Glan prism, the dye laser is tuned to the desired frequency, and a predetermined number of shots

(usually 10–20) is fired with the second harmonic of the ruby blocked and prevented from entering the cell. For these shots the average value of the ratio of the signal S from the signal channel to R, the signal from the reference channel, is determined—and called $(S/R)_0$. Subsequently, the block is removed and the same ratio (S/R) is obtained in the presence of I_L. The normalized change in this ratio is recorded and plotted as in Figs. 2(b) and 2(c) as a function of the dye laser frequency:

$$M=\frac{\Delta I_P}{I_P}=\frac{S/R-(S/R)_0}{(S/R)_0}\,. \tag{8}$$

The estimated error in the determination of $(S/R)_0$ and S/R is 0.5% and 1%, respectively, and could be improved by averaging more laser shots.

Having defined the measured quantity M, we go back to Eq. (5) and note that

$$S/R\sim\frac{I_P(d)}{I_P(0)}\,, \tag{9}$$

or, after normalization,

$$\begin{aligned}M&=\frac{S/R}{(S/R)_0}-1=e^{-\beta_{\rm eff}I_L(0)d}-1\\&\cong-\beta_{\rm eff}I_L(0)d\\&=[\beta_{T,c}l+(\beta_{T,l}-\beta_{R,l})(d-l)](1-R_L)I_L(0)\,.\end{aligned} \tag{10}$$

The measured spontaneous Raman line shape of the 3062-cm^{-1} line of benzene as measured on a Raman spectrometer is shown in Fig. 2(a). Details of the Raman measurements, and the determination of the absolute Raman cross section, are given in the Appendix, and will be described fully elsewhere.[15] The fitting procedure can be readily understood with reference to Fig. 2. The Raman line profile from Fig. 2(a) is scaled to fit the data points in Fig. 2(b) for benzene or 2(c) for the composite sample. The fitting parameters are then used to obtain the absolute TPA cross section as described below.

The spontaneous spectrum $\rho(\nu)$, where ν is the Raman shift in wave numbers, can be described by

$$\rho(\nu)=A\,S(\nu)+G\,, \tag{11}$$

where A is the integrated area of the measured Raman line (in arbitrary units), $S(\nu)$ is a normalized line-shape function, in principle unknown, and G is the background noise of this measurement. $\rho(\nu)$ can be scaled to fit M by two parameters B, C such that

$$M=C\rho(\nu)+B=CA\,S(\nu)+(CG+B)\,. \tag{12}$$

This is not a two-parameter fit, as M was measured and found to be flat to a large distance away from the Raman line peak, and thus the choice of B is not free. *C is the only scaling parameter.* On the other hand, Eq. (10) gives an expression for M in terms of β_R and β_T. For the case under consideration, β_T is more or less structureless so that we can integrate over the line shape. As follows from Eq. (7) the integral Ω of the Raman coefficient β_R can be calculated from the known Raman cross section according to

$$\Omega=\int\beta_R(\nu)\,d\nu=\frac{1}{hc^2n_P^2}\,\frac{1}{\nu_L\nu_P^2}\,\frac{N}{V}\,\frac{d\sigma}{d\Omega}\,. \tag{13}$$

The TPA coefficients are obtained from

$$\begin{aligned}\beta_{T,l}&=-\frac{(B/C)_l+G}{A}\,\Omega\,,\\\beta_{T,c}&=[(B/C)_l-(B/C)_c][(d-l)/Al]\,\Omega=D\Omega\,,\end{aligned} \tag{14}$$

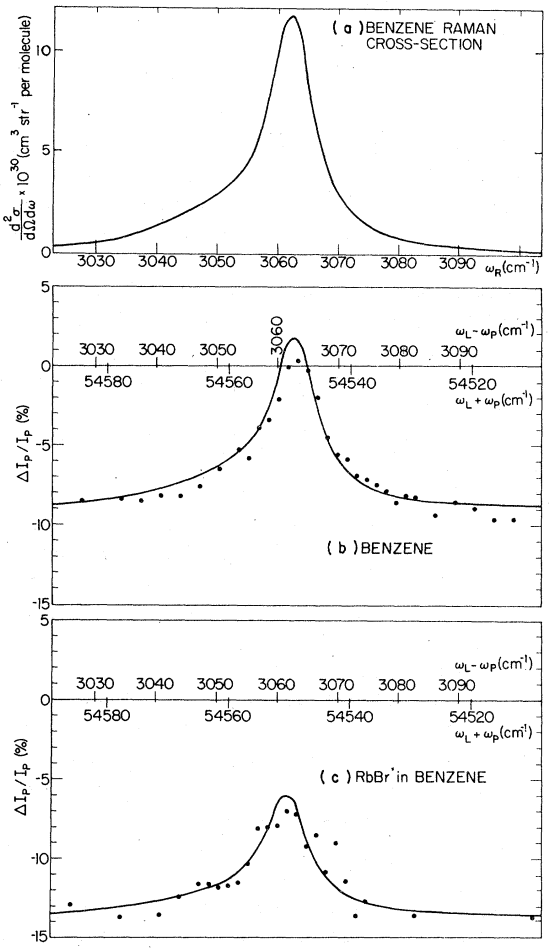

FIG. 2. (a) Benzene cross section as measured on the spectrometer, calibrated for excitation at 347.1 nm. (b) Benzene spectrum from (a) scaled to fit the measured points for a benzene cell. The vertical scale is the percentage attenuation of I_P. (c) Same as (b) for the composite sample of RbBr in benzene.

where B/C is the ratio of the fitting parameters for the liquid (l) and the crystal (c). As already mentioned before, d and l are the lengths of the cell and the crystal, respectively, while A is the measured integrated area of the Raman line in the units used in the fitting.

This fitting procedure, which is much easier to perform than to be described, results in a proportionality constant D that relates the absolute TPA coefficient of the crystal to the known integrated Raman coefficient of the liquid.

IV. RESULTS AND DISCUSSION

Figure 2 shows a set of experimental results used in calculating the TPA coefficient of RbBr. Figure 2(a) presents a Raman spectrum as taken on a Raman spectrometer. No attempt is made to describe the line by analytic functions, but instead, the fitting procedure uses the raw spectrum. In Fig. 2(b) we show the result of a run with a sample of benzene alone. One notes that at this energy range (6.7 eV or ≈180 nm) the benzene experiences TPA about the size of the Raman gain at the peak of the 3062-cm^{-1} line. This is a fortunate coincidence as it allows the increase of laser power without the occurrence of Raman oscillations arising from spontaneous scattering. Several other organic solvents—like acetone, acetic acid, and cyclohexane—were also studied but were found to have a much smaller TPA loss, so that they broke into oscillation at a relatively low laser power. The problem of self-focusing, which usually interferes with measurements of stimulated Raman gain due to the fact that the threshold for self-focusing is lower than that for stimulated Raman oscillations, is bypassed here. In our measurement we are interested in the relative size of the Raman gain and the TPA loss, and they both depend on the beam parameters in the same way. Thus, even if self-focusing occurs, the relative size of the two effects does not change. We tried to avoid self-focusing only to the extent of not having a measurable signal at ω_P at the signal channel in the absence of the probe beam. As is pointed out above, this is not a problem for benzene due to the high TPA loss, but was a problem for the other liquids which were therefore not used. Thus benzene is an ideal liquid sample for our method, both due to its being the best studied organic solvent and the availability of Raman cross sections, and due to the two-photon absorption in this energy range.

From Fig. 2(b) the TPA coefficient of benzene can be determined, and from Fig. 2(c), which is the result for a composite sample of RbBr in benzene, the TPA coefficient of the crystal can be derived.

To verify the authenticity of our measurements the following tests and experiments were performed: (a) The dependence of the measured M on the intensity I_L of the second harmonic was tested and found to be linear over the range of intensities used, e.g., up to $\Delta I_P/I_P = 12\%$ in benzene. For intensities much higher than that the Raman gain saturated. The linear dependence on the intensity I_L also insures that there is no contribution from higher-order processes like three-photon (two at ω_L and one at ω_P) absorption, or from generation of free carriers by two photons at ω_L followed by a subsequent absorption of a photon at ω_P. (b) A composite sample measurement was performed on NaCl in benzene. No measurable TPA due to NaCl was observed. None was expected due to the larger band gap in this crystal. (c) Color centers were created and were visible after a few laser shots. We found that for the crystals reported here they did not have any measurable effect on the linear absorption or the TPA coefficient even after several hundred shots at the same position. (d) In RbI the color centers had a significant effect on the linear absorption, and thus this crystal could not be used in the present study. (e) The total size of M was kept small so that point (a) holds and the lowest-order approximation for the exponential gain

$$\exp[-\beta_{\text{eff}} I_L(0) d] \approx 1 - \beta_{\text{eff}} I_L(0) d$$

could be used. We calculated the contributions from the next term in the expansion and from the depletion of I_L due to TPA at $2\omega_L$. Both effects together amount to less than a 2% correction for the values of β_T.

Our results for the TPA coefficients are summarized in Table I. The table also presents the proportionality constant D which is the result of our measurement, and is independent of the value for the Raman cross section $(d\sigma/d\Omega)$ which we derive from published data. In this work we use the value

$$\left(\frac{d\sigma}{d\Omega}\right)_{\parallel} = (190 \pm 30) \times 10^{-30}\ \text{cm}^2\,\text{sr}^{-1}\,\text{molecule}^{-1}$$

as the Raman cross section for scattering of the 3062-cm^{-1} line of liquid benzene excited by light of wavelength 347.1 nm. (For details on how this value is determined and the uncertainty in its determination see the Appendix.)

The only other published results for TPA coefficients in the uv are those of Liu *et al.*[8] These authors used the third (355 nm) and fourth (266 nm) harmonics of the Nd-YAlG fundamental, and obtained both the laser and probe beams from the

same laser. In their case $\omega_P = \omega_L = \omega$; the relevant $\chi^{(3)}$ term is $\chi^{(3)}(-\omega,\omega,\omega,-\omega)$ and the appropriate degeneracy is 3 [see Eq. (2a) and the following discussion]. Thus for the same material and the same $\chi^{(3)}$, our method will measure a TPA coefficient twice as large. A different way to look at the comparison of the two cases is by examining Eq. (1) in the limit of $\omega_P \to \omega_L$. In this limit the intensities of the two beams are not to be multiplied, but instead, one needs to add the (now interfering) electric fields and only then square for the intensity. The result is a factor of $\frac{1}{4}$, i.e., $I_P I_L \to \frac{1}{4} I_L^2$. The factor changes back to $\frac{1}{2}$ when account is taken of the fact that in this limit the total change of both beams is observed. Thus in the limit of $\omega_P = \omega_L$ the left-hand side of Eq. (1) should be changed:

$$\frac{\partial I_P}{\partial z} \to \frac{1}{2}\frac{\partial I_L}{\partial z} .$$

This difference between the two lasers and one laser case has often been overlooked in the past. Thus our 18.2×10^{-3} cm/MW for KI should be compared with twice the result of Liu *et al.*, or with 14.6×10^{-3} cm/MW. Our 11.3×10^{-3} cm/MW for RbBr corresponds to their 4.9×10^{-3} cm/MW. This is a good agreement considering that these are two independent absolute measurements done from totally different experimental approaches. Due to the error margins on the absolute values obtained from these measurements (±25% on ours, and ±65% on theirs) and the difficulties involved in performing these experiments, not much can be said about the significance of the difference in TPA coefficients for our nsec pulses and the psec pulses of Liu *et al.* It should be emphasized, however, that in spite of the vast (three orders of magnitude) difference in the size of the laser intensities involved, the total energy flux through the samples was similar (of the order of 100 mJ/cm^2) in both systems. Further investigation is needed to determine whether this agreement of results still holds for the case where a similar focusing is applied and the energy flux of the nsec system is much larger.

V. CONCLUSIONS

We have presented new measurements of uv TPA coefficients using the technique of internal calibration, the essence of which is a comparison of TPA and Raman processes. The results agree quite well with the only other published results in the two-photon energy range around 6.7 eV. It is pointed out that care should be taken when comparing results obtained in "one-beam techniques" to those obtained in "two-beam techniques," as under identical conditions the former will show TPA only half as big as the latter. We found that in this energy range benzene is an ideal standard liquid, as its inherent TPA prevents it from breaking into Raman oscillation.

The limitations of our method are in sensitivity and wavelength coverage. We estimate that the smallest TPA coefficient measurable to an accuracy of ±50% in this method is about 10^{-4} cm/MW, and could be achieved by tighter focusing of the beams. Since the method is very sensitive to alignment of the two beams, we do not believe that it could prove a viable approach for a broad frequency range, certainly not more than the range covered by one dye.

Based on the results of this work we propose, however, that for liquids the same internal calibration technique could be performed in a capillary tube or an optical fiber. If the two beams are confined to the liquid inside a long narrow capillary tube, their overlap is constant over most of the length of the tube and thus should be very insensitive to slight misalignment of the beams outside the tube as long as they are focused into it. Raman gain has been reported in optical fibers[16] for very low input powers. Thus the proposed method is expected to be very sensitive. Experiments to explore this possibility are under way in our laboratory. In this case two tunable dye lasers

TABLE I. TPA cross sections.

Material	Laser polarization	Surface normal	Proportionality[a] constant D (cm)	β_T (cm/MW)[b]
Benzene			0.0532	2.53×10^{-3}
KI	[001]	[100]	0.383	18.2×10^{-3}
KBr	[001]	[100]	0.167	7.98×10^{-3}
RbBr	[001]	[100]	0.274	11.3×10^{-3}

[a] See Eq. (14) for a definition of D.

[b] Based on the value $(d\sigma/d\Omega)_{\|} = (190+30)\times10^{-30}$ cm^2 sr^{-1} molecule^{-1} or $\Omega = 47.6\times10^{-3}$ MW^{-1}. See the Appendix for details.

will be used, enabling the investigation at any desired frequency range.

ACKNOWLEDGMENTS

We wish to thank Dr. S. Asher for use of the Raman spectrometer, Professor D. Latham for use of a calibrated lamp to calibrate the spectrometer, S. Maurici for polishing the crystals, and P. Liu and Professor N. Bloembergen for many helpful discussions and a critical reading of the paper. This work is supported in part by the Joint Services Electronics Program under Contract N00014-75-C00648.

APPENDIX

We could not find a single report on an absolute cross-section measurement of the 3062-cm^{-1} line of benzene. Several measurements were reported for the 992-cm^{-1} line at the following excitation wavelengths: 632.8 nm,[17,18] 532.0,[19] 514.5,[18,20] 488.0,[18,21] 435.8,[18] and 337.1 nm.[20]

All the quoted measurements, with the exception of that at 337.1 nm, were performed with cw lasers. Most of them were based on comparison of the Raman scattered light to a light source of known brightness. The cross section determination at 337.1 nm was done with a pulsed N_2 laser. It was based on comparison of the 992-cm^{-1} line of benzene to a rotational Raman line of molecular hydrogen. The cross section for the rotational Raman transition was calculated from the linear polarizability tensor. The value for benzene was then obtained in a rather indirect way via a Raman line of gaseous and liquid cyclohexane and local field corrections.

In addition, Ziegler and Albrecht[22] proposed two extrapolation formulas for the Raman cross sections of the 992- and 3062-cm^{-1} lines of benzene for different excitation wavelengths.

We measured the relative strength of several benzene lines (including the 922- and 3062-cm^{-1} lines) at the following excitation wavelengths: 632.8, 580.6, 514.5, 488.0, 457.9, and 351.4 nm, and the results will be published elsewhere.[15] The 351.4-nm line is a uv Ar-ion laser line that is the closest to the required excitation wavelength of 347.1 nm. We used the published absolute cross sections of the 992-cm^{-1} line at 632.8, 514.5, and 488 nm, and arrived at the absolute cross section for excitation at 351.4 nm in two ways: (a) by use of the extrapolation formula given by Ziegler and Albrecht[22]; (b) by use of our relative measurements of the cross sections of the 922-cm^{-1} line at these excitations. Both methods agree to within 10%, and the value we used for $d\sigma/d\Omega$ of the 922-cm^{-1} line of benzene at excitation of 351.4 nm is $(150 \pm 30) \times 10^{-30}$ $cm^2\,sr^{-1}$ $molecule^{-1}$. We measured the 3062-cm^{-1} line to be 1.2 times stronger (integrated intensity) than the 922-cm^{-1} line at excitation of 351.4, and together with the extrapolation formula for the 3062-cm^{-1} line ($\sim\lambda^{-4}$) we arrive at the value we use at this work:

$$\left(\frac{d\sigma}{d\Omega}\right)^{3062} = (190 \pm 30) \times 10^{-30}\,\mathrm{cm^2\,sr^{-1}\,molecule^{-1}}.$$

We used the above absolute cross sections as they were consistent with our relative measurements and the extrapolation formulae. The published value for the 992-cm^{-1} line excited at 337.1 nm seems to be too large by a factor of about 1.6 and was not used.

---

*Permanent address: Dept. of Chemical Physics, Weizmann Institute of Science, Rehovot, Israel.

†On leave from Physikalisches Institut der Universitat Koln, Zulpicher Strasse 77, 5000 Koln 41, Federal Republic of Germany.

[1] W. Kaiser and C. G. B. Garrett, Phys. Rev. Lett. 7, 229 (1961).

[2] A. J Twarowski and D. S. Kliger, Chem. Phys. 20, 253 (1977).

[3] P. M. Johnson, J. Chem. Phys. 64, 4142 (1976).

[4] I. M. Catalano, A. Cingolani, and A. Minafra, Phys. Rev. B 9, 707 (1974).

[5] J. M. Worlock, in *Laser Handbook*, edited by F. T. Arecchi and E. O. Schulz-Dubois (North-Holland, Amsterdam, 1972); H. Mahr, in *Quantum Electronics*, edited by H. Rabin and C. L. Tang (Academic, New York, 1975); V. I Bredikhin, M. D. Galanin, and V. N. Genkin, Sov. Phys -Usp. 16, 229 (1973).

[6] R. L Swofford and W. M McClain, Rev Sci. Instrum. 46, 246 (1975).

[7] R. W. Hellwarth, Prog. Quantum Electron. 5, Part 1 (1977).

[8] P. Liu, W. L. Smith, H. Lotem, J. H. Bechtel, N. Bloembergen, and R. S. Adhav, Phys. Rev. B 17, 4620 (1978).

[9] M. D. Levenson and N. Bloembergen, J. Chem. Phys. 60, 1323 (1974).

[10] R. T. Lynch, Jr., and H. Lotem, J. Chem. Phys. 66, 1905 (1977).

[11] S. D. Kramer and N. Bloembergen, Phys. Rev. B 15, 4654 (1976).

[12] H. Lotem and C. B. deAraujo, Phys. Rev. B 16, 1711 (1977).

[13] C. B. deAraujo and H. Lotem, Phys. Rev. B 18, 30 (1978).

[14] N. Bloembergen, Am. J. Phys. 35, 989 (1967);

R. Loudon, *The Quantum Theory of Light* (Clarendon, Oxford, 1973), Chap. 12.
[15]Y. Prior, S. Asher, H. Vogt, and R. Pawlik (unpublished).
[16]J. Stone, Appl Phys. Lett. 26, 163 (1974) and references therein.
[17]T. C. Damen, R. C. C. Leite, and S. P. S. Porto, Phys. Rev Lett. 14, 9 (1965).
[18]Y. Kato and H. Takuma, J. Chem. Phys. 54, 5398 (1971); J. Opt. Soc. Amer. 61, 347 (1971).
[19]A. Owyoung and P. S. Peercy, J. Appl. Phys. 46, 674 (1977).
[20]N. Abe, M. Wakayama, and M. Ito, J. Raman Spectosc. 6, 38 (1977).
[21]J. G. Skinner and W. G. Nilsen, J. Opt. Soc. Am. 58, 113 (1968).
[22]L. Ziegler and A. C. Albrecht, J. Chem. Phys. 67, 2753 (1977).